

# Science White Paper for LSST Deep-Drilling Field Observations

## Mapping the Milky Way’s Ultracool Dwarfs, Subdwarfs, and White Dwarfs

S. Dhital (Vanderbilt), P. Thorman (UC–Davis), J. J. Bochanski (Penn State), P. Boeshaar (UC–Davis), A. J. Burgasser (UC–San Diego), P. A. Cargile (Vanderbilt), K. R. Covey (Cornell), J. R. A. Davenport (Washington), L. Hebb (Vanderbilt), T. J. Henry (Georgia State), E. J. Hilton (Washington), Z. Ivezić (Washington), J. S. Kalirai (STSci), S. Lépine (AMNH), J. Pepper (Vanderbilt), S. J. Schmidt (Washington), K. G. Stassun (Vanderbilt), L. M. Walkowicz (UC–Berkeley), A. A. West (Boston Univ)

### Contact Information for Lead Author/Authors:

Saurav Dhital, Department of Physics & Astronomy, Vanderbilt University, 6301 Stevenson Center, Nashville, TN, 37235. Email:saurav.dhital@vanderbilt.edu. Ph: (610) 368–8430

Paul Thorman, Department of Physics, University of California, One Shields Ave., Davis, CA 95616. Email: thorman@physics.ucdavis.edu. Ph: (505) 449-7864

## 1 Science Goals

### 1.1 Concise List of Main Science Goals

- 1. Identifying and characterizing L and T dwarfs:** While the main LSST survey should detect nearly 40,000 L and T dwarfs, the vast majority of late-L and T dwarfs will only be detected in the  $z$  and  $y$  bands. However, unambiguous separation of these local sources from extragalactic sources and their full characterization requires detection in at least the  $i$ ,  $z$ , and  $y$  bands. Deep exposures to extend LSST’s  $i$  band depth to match the  $z$  and  $y$  bands will allow us to establish the properties of the ultracool dwarfs. The results can possibly be extended to characterize the ultracool dwarfs with only  $z$  and  $y$  detections in the main LSST survey. These deep exposures will also be crucial in identifying the fast-moving stellar sources.
- 2. Mapping the low-mass subdwarfs in the Milky Way halo:** Mapping the low-mass stars in halo of the Milky Way in spatial, kinematic, and metallicity spaces will require deep coverages in the  $g$ ,  $r$ , and  $i$  band. While expensive, such a study would allow for a synoptic tomography of the Milky Way using the most abundant, yet intrinsically faint, members of the Milky Way stellar population.
- 3. Calibrating magnetospheric structure and angular momentum evolution in M, L, and T dwarfs and the cloud properties in L dwarfs:** Temporal coverage of intermediate-age open clusters and nearby young populations will allow for the study of (i) magnetospheric structure and angular momentum evolution in M, L, and T dwarfs, (ii) flare rate in M and L dwarfs, and (iii) the cloud properties of L dwarfs.
- 4. Identifying benchmark brown dwarf systems:** Calculating the mass, age, or metallicity of isolated brown dwarfs (BD) is not currently possible as the models cannot account for the clouds present in their atmospheres. Hence, benchmark systems need to be identified. DDF can address the issue by identifying benchmark systems in three ways: (i) the high contrast ratio of coadded images will allow for identification of BDs in binary systems with a subgiant primary, which can provide ages accurate to  $\sim 10\%$ , (ii) identification of rare, BD+BD eclipsing binaries in open clusters of known ages and metallicities, and (iii) identification of an additional  $\sim 10$  BD+BD eclipsing binaries, in addition to the  $\sim 20$  expected in the main LSST survey.

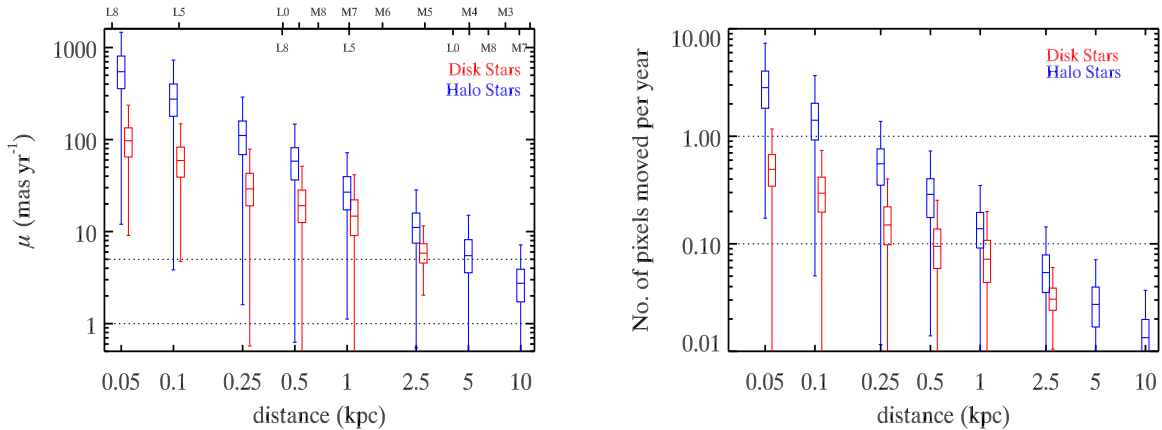


Figure 1 **(a)** The box-and-whisker distribution of simulated proper motions of disk (Bochanski et al. 2010; Bond et al. 2010) and halo stars (Bond et al. 2010) as a function of heliocentric distance for a LSST field looking towards the South Galactic Pole. The proper motions of the majority of the disk and halo stars will be measured in 3 and 10 yrs, respectively (detection limits shown by the dotted lines). The upper x-axes show the latest type star that will be detected at the distance in a single epoch in the main LSST survey ( $i = 24$ ; outer ticks) and in our proposed DDF observations ( $i = 28.9$ ; inner ticks). The DDF observations will allow us to construct a spatial and kinematic map of the Galaxy to  $\sim 500$  pc complete to late-type L dwarfs and to  $\sim 2500$  pc complete to mid-type M dwarfs. **(b)** The high proper motion stars will be moving too fast to be properly coadded in the main LSST survey; in fact, the majority of stars within  $\sim 500$  pc will move more than 1 pixel over the 10 yr survey length. Hence, the faintness limit for fast-moving stellar sources is actually brighter than the survey limits, which underscores the role of DDF in mapping the Galaxy.

## 1.2 Details of Main Science Goals

### 1.2.1 Identifying and Characterizing L and T dwarfs

No study of Galactic structure and properties will be complete without a census of the substellar population. The very wide-field surveys of DENIS (e.g. Delfosse et al. 1999), 2MASS (e.g., Kirkpatrick et al. 1999; Cruz et al. 2003, 2007), SDSS (e.g., Chiu et al. 2006; Schmidt et al. 2010), and UKIDSS (e.g., Deacon et al. 2009) have identified over 1000 brown dwarfs<sup>1</sup> of types L and T based on the optical and infrared broadband colors and various absorption features. Since these objects are intrinsically faint ( $M_i > 16$  mag; Hawley et al. 2002), nearly all known early-L dwarfs are within  $\sim 120$  pc and mid-late L and T dwarfs are within  $\sim 50$  pc of the Sun (e.g., Reid et al. 2003, 2008; Schmidt et al. 2010), making the Galactic distribution (such as the disk scale height and length) difficult to determine. While this problem can be overcome by using deeper data sets that probe significantly further into the disk, limited observing time and poor detection efficiency have restricted all studies to using extremely narrow fields-of-view and/or single lines-of-sight (e.g., Ryan et al. 2005; Pirzkal et al. 2005, 2009). Naturally, this results in over-simplified models (such as a single disk component), large uncertainties on the model parameters (such as the vertical scale height), and significant variation between the authors.

With a coadded faintness limit of  $z \sim 26.2$ , the main LSST survey is in a position to identify tens of thousands of L and a few thousand T dwarfs (LSST Science Collaborations et al. 2009). However, there are questions as to whether they can be unambiguously identified as stellar/substellar sources and further characterized as L and T dwarfs at  $z = 23.3\text{--}26.2$ , the regime where they are only

<sup>1</sup><http://dwarfarchives.org>

detected in coadded images. First, due to their intrinsic faintness, a significant number of L dwarfs and the vast majority of T dwarfs will only be detected in the  $z$  and  $y$  bands, even in the coadded images, requiring parallax and/or proper motions to unambiguously separate them from extragalactic sources, neither of which will be available for these sources. Second, the majority of dwarfs, as well as a fraction of halo subdwarfs, within  $\sim 1000$  pc will be moving fast enough to change their position by  $\sim 1$ – $6$  pixels in the 10 yr survey lifetime, as shown in Figure 1b. Hence, while there are expected to 5–10 times more stars—with the exact number dependent on the line-of-sight—at  $z = 23.3$ – $26.2$  compared to  $z < 23.3$  (LSST Science Collaborations et al. 2009), many of them will not be identified<sup>2</sup> These photometric limitations will introduce significant biases in the measured number density and luminosity function parameters.

The Deep Drilling Field observations (DDFs) can address the above shortcomings by observing to fainter magnitudes in a single epoch, or within a timespan that allows for the images to be properly coadded. Given the constraints for the DDF, the most efficient way to unambiguously identify the largest possible number of L and T dwarfs is to augment observations in the  $i$  band so as to reach the same depths in the  $z$  and  $y$  bands. While this strategy will not lead to an increase in the total number of L and T dwarfs detected, it will at least double the number of late-L and T dwarfs identified based on three-band detection and proper motions. A large sample of L and T dwarfs would allow us to probe their age and metallicities as a population using Galactic height.

### 1.2.2 Mapping the Low-mass Subdwarfs in the Milky Way Halo

A deep survey ( $r = 27.0$  or fainter) would reveal the low-mass stellar component of the Galactic halo to unprecedented distance and depth. Low-mass stars in the halo are cool, metal-poor dwarfs, which are spectroscopically classified as “M subdwarfs”. Based on photometric data from SDSS, it is found that M subdwarfs have distinct colors in a  $(g - r)$  vs.  $(r - i)$  diagram (Lépine & Scholz 2008), and can be separated from metal-rich M dwarfs by color (Figure 2a). In particular, it should be noted that the coolest subdwarfs also show the largest color differences as a function of metallicity, to such an extent that the  $(g - r)/(r - i)$  color ratio can be used to obtain a relatively reliable metallicity estimate in late-type M subdwarfs (Lépine et al. *in prep.*) provided that  $gri$  photometry can be measured to an accuracy of  $\pm 0.05$  mag. This remarkable property would allow one to obtain abundance estimates in distant late-type M subdwarfs *based on gri photometry alone*.

The typically large proper motions of the old-disk and halo M subdwarfs also helps in their identification and unambiguous separation from extragalactic sources with similar colors. A simulation of the M subdwarf population from the galactic thick disk and halo (Figure 2b) shows that within 2.5 kpc (5.0 kpc) of the Sun, the majority of M subdwarfs would have proper motions in excess of  $20 \text{ mas yr}^{-1}$  ( $10 \text{ mas yr}^{-1}$ ). The detection of low-luminosity M subdwarfs over such a large distance range however requires a very deep survey. Figure 2c shows the predicted color and magnitude range for M subdwarfs with proper motion  $\mu > 20 \text{ mas yr}^{-1}$  from the same simulation; the numbers are those expected from a 1 sq. deg. field of view at high Galactic latitude. The field contains  $\approx 3,000$  stars which extend to  $r \simeq 28$ . Over 2/3 of the stars are fainter than  $r = 24$  and will be too faint to be detected in the normal LSST survey. Most importantly, *the regular survey will miss most of the all-important late-type M subdwarfs ( $g - i > 2.7$ ) whose metallicities can be estimated by color*. Deeper imaging to  $r = 27$ – $28$  would detect thousands of late-type M subdwarfs from the halo in a single 1 sq. deg. field. This would yield reliable kinematics and abundance patterns for an unprecedented number of low-mass halo stars. As a result we would be able to trace the structure and metallicity of the Galactic halo with its most abundant stellar members.

Since the halo M subdwarfs are distributed all over the sky, any line-of-sight would yield signifi-

---

<sup>2</sup>When there is evidence of the presence of a source, the multifit algorithm should be able to recover the objects by fitting multiple exposures simultaneously; but that will only be true for a small subset.

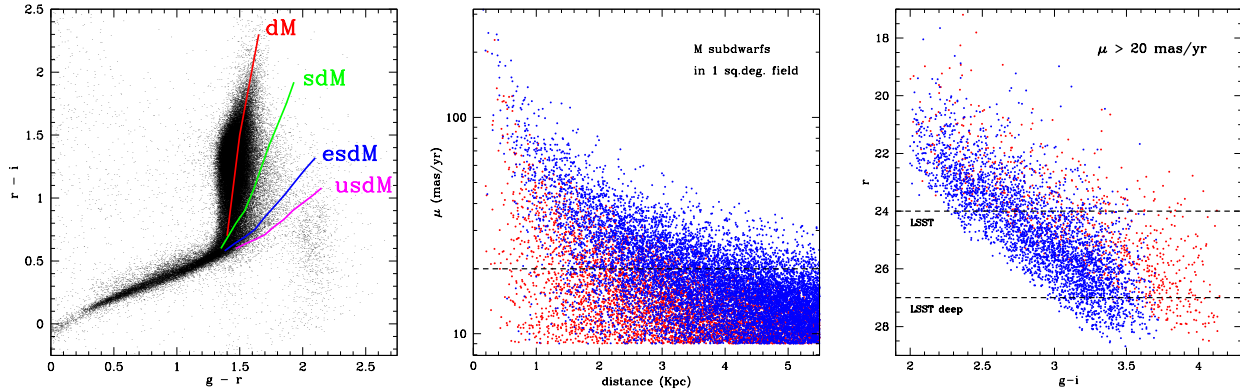


Figure 2 (a) Mean color-color distribution of M dwarfs and subdwarfs, plotted for the four metallicity classes: dwarfs (dM, with  $\log Z \approx 0.0$ ), subdwarfs (sdM,  $\log Z \approx -0.7$ ), extreme subdwarfs (esdM,  $\log Z \approx -1.3$ ), and ultrasubdwarfs (usdM,  $\log Z \approx -2.0$ ). The sdM are typically members of the old/thick disk, while esdM and usdM are kinematically associated with the Galactic halo. A typical color-color distribution for SDSS point sources is shown for comparison (black dots). (b) Proper motions of M subdwarfs as a function of their distance from a simulation of a high Galactic latitude, 1 sq. deg. field based on the predicted local thick disk and halo populations; halo stars are plotted in blue, thick disk stars in red. (c) Apparent magnitude as a function of color for a the subsample of M subdwarfs with proper motion  $\mu > 20 \text{ mas yr}^{-1}$  in a simulation of stars detected in a 1 sq. deg. field at high Galactic latitude. Late-type M subdwarfs,  $g - i > 2.7$ , can be detected only in a deep survey reaching to  $r = 27\text{--}28$ . Note that the proper motion cut selects for the nearest (and hence relatively brightest) sources. A lower proper motion cut would yield larger numbers of generally more distant stars, but these would be even fainter than those on display here.

cant numbers of detections. The only exception would be a field close to the plane of the Milky Way, where extinction and reddening would be a problem. Ideally, one would want to spread the deep fields at different lines-of-sight in order to probe the M subdwarf density, kinematics, and metallicity over different sections of the local halo.

### 1.2.3 Calibrating the Magnetospheric Structure and Angular Momentum Evolution in M and L Dwarfs and the Cloud Properties in L Dwarfs

**Angular momentum evolution in fully convective stars:** Low-mass stars ( $M \lesssim 0.4 M_{\odot}$ ; Chabrier & Baraffe 1997) are fully convective and hence lack the shear responsible for generating and sustaining the magnetic fields present in the solar-type stars. Numerical simulations have indicated that the dynamo in fully convective stars are produced by small-scale, intermittent flows at the surface and weaker, large-scale flows in the interior (e.g., Browning 2008). While the evolution of rotational periods (the observational signature of the modulation of starspots) of solar-type stars, caused by magnetic field-induced stellar winds that carry away angular momentum, has been well studied (e.g., Barnes 2003, 2007, 2010; Meibom et al. 2009), our knowledge is still sparse for low-mass stars. Recent observations indicate a geometric change in the magnetic fields at the fully convective boundary (e.g., Donati et al. 2008; Morin et al. 2008, 2010); however, the effect of the change on stellar winds and rotational evolution is not yet clearly understood.

Observationally, the intrinsic faintness of the low-mass stars makes empirically constraining their rotational evolution difficult. The primary sources of low-mass stellar rotation periods currently come from surveys of young, pre-main-sequence open clusters ( $<100 \text{ Myr}$ ; e.g., Stassun et al. 1999; Herbst et al. 2001; Lamm et al. 2005; Scholz et al. 2009) and nearby field samples with relatively

poor age constraints (e.g., Irwin et al. 2011). Although the data sets are limited, preliminary findings show a large range of rotation periods (from  $<1$  day to  $>100$  days; Irwin et al. e.g., 2011) and an age-dependent spin-down, albeit at a different rate than in solar-type stars. However, the lack of rotation periods in older clusters ( $>100$  Myr) is hampering a more detailed understanding of rotational evolution in low-mass stars.

The high cadence, photometric depth, and large field of view of the DDF will make it a powerful data set to empirically characterize low-mass stellar rotational evolution. Several open clusters in the LSST footprint are at distances ( $<1$  kpc) and ages ( $>100$  Myr) perfectly suited for deep monitoring campaigns of low-mass stellar members, and would likely yield a significant number of rotation periods. Examples of possible target clusters are Blanco 1 (age: 140 Myr, distance: 250 pc), NGC 3532 (300 Myr, 450 pc), NGC 2527 (500 Myr, 600 pc), and IC 4651 (1 Gyr, 900 pc). DDF monitoring of these clusters will have a cadence necessary ( $\sim 70$ – $100$  epochs in  $\sim 30$  days) to detect rotation periods of rapidly rotating stars (period  $\lesssim 15$  days) that would otherwise not be detected in the main LSST survey. In fact, the short rotation periods from the DDF coupled with longer periods measured from main LSST survey data will provide an extensive data set that will be sensitive to a wide range of rotation periods, thus providing a more complete description of rotation period distributions of these open clusters.

**The flare rate in M and L dwarfs:** The activity in M dwarfs, as traced by incidence of H $\alpha$  emission, dramatically rises to  $\gtrsim 50\%$  around the fully convective boundary and to 100% for the late-M and early-L dwarfs (Gizis et al. 2000; West et al. 2004, 2008, 2011), indicating a different mechanism of magnetic field generation than the solar-type stars. This fraction drops off for later-type L dwarfs, reflecting a decoupling between magnetic field lines and an increasingly neutral photosphere (Mohanty et al. 2002), and among older populations of M dwarfs, reflecting a gradual spin-down of these objects through stellar winds (West et al. 2006). However, flaring emission from radio to X-ray wavelengths is seen even among seemingly inactive M and L dwarfs (Reid et al. 1999; Liebert et al. 2003; Schmidt et al. 2007), indicating the presence of kilogauss magnetic fields (Reiners & Basri 2007). Tracking the frequency and luminosity of flares from M and L dwarfs in deep pointings through high-cadence and long-term *griz* photometric monitoring will allow us to examine the temporal evolution of magnetic field topologies among late-M and L dwarfs where quiescent indicators are absent. Moreover, by probing M and L dwarfs at large scale heights, the DDF will be able to assess any correlations between magnetic variability, mass, and age and make a robust assessment of the low-mass stellar contribution to the X-ray and UV background.

Although the LSST universal cadence will likely yield many hundreds of serendipitous flare observations every night (Hilton et al. 2010), the DDFs will improve flare science through both the much larger number of observations, as well as through the increased depth. Flares observed in the universal cadence will be useful in a statistical sense only because individual stars are very unlikely to show flaring in more than a few epochs (Kowalski et al. 2009). The larger number of epochs in the DDFs, particularly in *g*, will allow rough characterization of the flare rates of individual stars. These rates will be especially useful in understanding the magnetic field generation of low-mass stars when combined with measured rotation periods. Very large flares on distant low-mass stars (too faint to be seen in quiescence) may appear as optical transients in as many as 10% of *u* images (Hilton et al. 2011, *in prep.*). In addition, the role of DDFs identifying the transients as M/L dwarfs from other exotic Galactic and extragalactic sources will be crucial.

**Cloud variability in L dwarfs:** In addition to magnetic flaring, L dwarfs also exhibit photometric variability arising from the inhomogeneous distribution of condensate clouds in their photospheres. These clouds form as a consequence of low temperatures ( $T_{\text{eff}} < 2000$  K), vertical mixing, grain growth, and gravitational settling, resulting in a spectrum of grain sizes and heterogeneous grain compositions (e.g. Ackerman & Marley 2001; Burrows et al. 2006; Helling et al. 2006, 2008). Ground-based studies of nearby, bright L dwarfs have detected 1–10% brightness variations at op-

tical and near-infrared wavelengths, as well as spectral variations associated with key absorbers such as TiO, FeH, CrH, and H<sub>2</sub>O (e.g., Tinney & Tolley 1999; Bailer-Jones & Mundt 1999, 2001; Kirkpatrick et al. 2000; Koen 2003, 2005; Goldman 2005). Periodic variations with timescales on the order of hours reflect the rapid rotational velocities measured for these sources, but changes in amplitudes and phases over multiple rotation periods hint at cloud evolution (weather) and/or differential rotation. The DDF will greatly expand on these intriguing indications by providing a considerably larger sample of sources measured to uniform accuracy, at a cadence matched to the rotational periods, and over timespans can probe cloud evolution over many rotation periods. Moreover, measurement of variability in L dwarfs to large scale heights will allow us to explore the connection between cloud structure, mass, age, and metallicity, information that is critical for burgeoning 3D models of cloudy atmospheres in brown dwarfs and exoplanets (e.g., Freytag et al. 2010). In addition, the rotation periods inferred from cloud variability measurements will probe the angular momentum evolution of these objects over the age of the Galaxy, allowing us to understand the role (or absence) of stellar winds and potentially extend stellar gyrochronology relations down to and below the substellar limit (Barnes 2003, 2007; Reiners & Basri 2008).

#### 1.2.4 Identifying Benchmark Brown Dwarf Systems

The last fifteen years or so have seen the identification of more than 700 brown dwarfs and 1200 exoplanets. The atmospheres of these low mass, ultracool objects are highly complex and suffer from a variety of poorly understood processes (e.g., Allard et al. 2001; Saumon et al. 2007). This means that the models are far from perfect, and as a result they struggle to accurately predict the observational properties of these objects. As such it is not currently possible to calculate the age, mass, or metallicity accurately for a brown dwarf in the field. What is needed is a method of calibrating the models. This can be done through the identification of benchmark objects that have independently derived properties. Currently there are only a small number of ultracool objects that can be used as benchmarks, the majority of these are either young (<1 Gyr), or have large uncertainties on their properties. This number decreases dramatically at ages of >2 Gyr and to date only one ultracool object with an age of >4 Gyr has been identified (LSPM 1549B; Day-Jones et al. 2011) leaving the majority of the age range of the galactic disk unprobed.

**Subgiant+BD binaries:** *Ultracool companions as members of binary systems, particularly those containing a primary star with well-defined properties, is the ideal hunting ground for these benchmark objects.* For the majority of main-sequence stars after  $\sim 1$  Gyr, their ages are usually highly uncertain due to the convergence of evolutionary models on the main sequence (e.g., Girardi et al. 2000; Yi et al. 2001). However, the later stages of stellar evolution provide more accurate ages because of the rapidity of the star’s evolution. In particular, the subgiant phase can provide ages accurate at the 10% level (Thorén et al. 2004) as well as provide metallicity and accurate distance information for the ultracool companion.

With DDF we will be able to obtain coadded images with very high contrast ratios in order to identify very faint, substellar companions to known subgiants in our target fields. These highly rare benchmarks will thus be able to address the problems currently faced by models that overestimate the temperature of BDs with measured dynamical masses (e.g., Dupuy et al. 2009; Liu et al. 2010).

**BD+BD eclipsing binaries:** Prsa, Pepper, & Stassun (2011) have studied the science yield of LSST for eclipsing binaries (EBs). They find that the main survey will have good sensitivity to EBs with  $r < 20$  and with periods ranging from 0.1 days to  $\sim 200$  days but will be especially good for periods  $\lesssim 10$  days. This sensitivity arises from the long duration of the main survey, which permits a sufficient number of data points in eclipse to be obtained over the course of the survey lifetime. The vast majority of the detected EBs will be in the field, not associated with clusters or stellar associations. Indeed, at present, the number of benchmark-grade EBs that are members of clusters or associations numbers fewer than 20. Such EBs are particularly important because not only are

the fundamental parameters of the EB determined (masses, radii, temperatures, luminosities) but in addition an independent age constraint can be determined from the main sequence turnoff and/or from the white dwarf cooling sequence. DDF will permit clusters to be specifically targeted and, importantly, will allow the EBs in these clusters to be identified early in the LSST survey.

In addition, there is at present only one known EB consisting of two brown dwarfs (Stassun et al. 2006, 2007) which provides direct measurements of the brown dwarf masses, radii, gravities, temperatures, and luminosities. While main LSST survey should find  $\sim 15$  late-M and  $\sim 5$  L type BD+BD EBs, the ten DDF fields could augment another  $\sim 10$  such EBs if  $r = 27\text{--}28$  is reached for all ten fields.

### 1.3 Supplementary Science

**Mapping the Galactic mass budget & star formation episodes as a function of time:** The LSST DDFs will uncover the stellar graveyard of our Galaxy. Over 97% of all stars eventually end their lives passively, shedding away their outer layers and forming low mass white dwarfs. Given the star formation history of the Galactic halo, an appreciable mass of the Galaxy is tied up in these remnants. The current census of the Galactic white dwarf population has been greatly informed by SDSS and includes a few tens of thousands of stars. LSST’s general survey will expand this to several million stars but still will not reach the faintest objects and therefore leave a gaping hole in our understanding of the Galactic mass budget. For example, a 12 Gyr old white dwarf will have an apparent magnitude of  $V = 30$  at a distance of 5 kpc. Given the rising luminosity function of white dwarfs with magnitude, constraints on the normalization of scaling relations related to the baryonic density of our Galaxy will require ultra-deep imaging surveys to identify the faintest white dwarfs out to substantial distances.

A census of faint white dwarfs in the nearby halo will also establish an unprecedented white dwarf luminosity function. As these stars cool predictably with time, the luminosity function holds important clues to the star formation history of the progenitor population. For example, the truncation in the white dwarf luminosity function has been inverted to yield the age of the Galactic disk (e.g., Oswalt et al. 1996). With the DDFs, we will perform an analogous study of the Galactic halo, and therefore, independently measure when the first baryonic structure formed in the Milky Way. A direct comparison of this luminosity function with that established now for several nearby globular clusters can also set limits on the timescale of when the globular cluster population formed relative to the field stars.

**Constraining the L dwarf scale height and luminosity function:** As discussed in Section 1.2.1, DDF has the potential to detect and characterize tens of thousands of L and T type dwarfs. While they might not be as numerous as the more-massive M dwarfs, it is imperative that we understand their density and kinematic distribution to get a comprehensive picture of the Milky Way. Figure 1a shows that with *izy* photometry for all objects to  $i = 28.9$  and  $z = 24.9$ , we can detect a “complete” sample of early-L dwarfs to  $\sim 3900$  pc and late-L dwarfs to  $\sim 500$  pc, along with their proper motions. This will allow us to measure the scale height for L dwarfs as well as model it with two disk components. While kinematic studies have indicated that the distribution of early-L dwarfs (which are mostly stellar) is not much different from that of the M dwarfs (Schmidt et al. 2010; Bochanski et al. 2010), there should be an observed deficiency of mid-to-late L dwarfs at larger Galactic heights because older substellar objects will have cooled sufficiently to be in the T dwarf regime (e.g., Burrows et al. 2001). A precise measurement of this deficiency will be crucial in calibrating the cooling timescales of these objects, where the ages, of an ensemble of L and T dwarfs, would be calculated based on their height above/below the Galactic Plane.

## 2 Description of Proposed LSST Observations

### 2.1 List of Proposed Fields

1. South Galactic Pole (plus Blanco 1), J2000 00<sup>h</sup> 53<sup>m</sup>, -26° 33'
2. Galactic Anti-Center ( $l = 180$ ,  $b = -30$ ), J2000 04<sup>h</sup> 02<sup>m</sup>, 11° 01'
3. One of the following three open clusters:
  - (a) NGC 3532, J2000 11<sup>h</sup> 05<sup>m</sup>, -58° 44'
  - (b) NGC 2527, J2000 08<sup>h</sup> 03<sup>m</sup>, -28° 01'
  - (c) IC 4651, J2000 17<sup>h</sup> 25<sup>m</sup>, -49° 56'

### 2.2 Motivation for Proposed Fields

There are two primary considerations for field choices: (i) avoid the Galactic bulge and disk to reduce the likely contamination caused by higher-mass stars being reddened and extinguished due to dust and (ii) choose lines-of-sight where the radial velocity is approximately zero—as happens for stars towards the Galactic South Pole or the Galactic Center and Anti-center—so that the kinematic distributions can be constrained from proper motions alone (e.g., Ivezić et al. 2008). Both suggest high latitude fields; however, ultracool dwarfs are more likely to be found near the disk due to a higher number density and cooling with age. While the DDF field-of-view is relatively large, mapping the ultracool dwarfs in spatial, kinematic, and metallicity space will definitely need multiple lines-of-sight so as to avoid local substructure. These factors recommend at least the South Galactic Pole and  $l = 180^\circ$ ,  $b = -30^\circ$  field be imaged to appropriate depths in the *griz* bands. Two fields are needed to robustly constrain the spatial, kinematic, and metallicity distribution of subdwarfs and ultracool dwarfs in the Galaxy.

As for the open cluster fields, we have chosen four open clusters of intermediate ages (100–1000 Myr) and at distances suited for deep photometric monitoring of the low-mass members ( $\lesssim 1$  kpc) with LSST. As one of four candidate clusters, Blanco 1, lies along the South Galactic Pole, we only need one of the three other clusters. As these clusters can be chosen based on other DDF science goals, we leave it to the committee to select the second open cluster field from the three suggestions, as is convenient for other DDF science goals.

Finally, we note that all of our proposed fields can be combined with other science goals, either Galactic and extragalactic.

### 2.3 Observing Plan, Cadence, Filters, and Expected Depth

We have structured our observation plans into three mini-surveys based on filters and cadences required for the various science goals discussed in Section 1: (i) a deep subdwarf survey which requires deep imaging in the *gri* bands, (ii) a deep brown dwarf survey which requires deep imaging in the *i* band, and (iii) a photometric variability (due to starspots and/or clouds) survey that requires frequent *izy* imaging. We have recommended three fields for DDF observations, with each field serving at least two of the three mini-surveys. Tables 1, 2, and 3 summarize the three surveys and the time needed for each of them. We are recommending deep imaging the DDFs in the *gri* bands to match main survey’s one-year depths in the *z* band ( $\sim 24.9$  AB mag) for low-mass dwarfs and subdwarfs. As discussed in Sections 1.2.1 and 1.2.2, *izy* coverage is essential to identify L and T dwarfs and *gri* coverage is needed to characterize the halo subdwarfs.

Given the extreme red nature of the L and T dwarfs, a  $5\sigma$  depth in *i* of 28.9 mag (AB) would be required to detect all varieties of these objects. As proper motions can be calculated from *zy* band

Table 1. Field 1 (South Galactic Pole & Blanco 1)

	Time (s)	No. of exp. per night <sup>a</sup>	No. of nights per year <sup>b</sup>	No. of years per survey <sup>c</sup>	Total (ks)
<i>Deep subdwarf survey</i> (assuming $g_{AB} = 30$ , $r_{AB} = 28$ )					
Exposure time: $g$	120	25	30	10	900 ks
Exposure time: $r$	120	2	30	10	72 ks
Readout time	2	27	30	10	15 ks
Filter change	45	1	30	10	13.5 ks
<i>Deep brown dwarf survey</i> ( $i_{AB} = 28.9$ )					
Exposure time: $i$	120	25	30	3	270 ks
Readout time	2	25	30	3	4.5 ks
Photometric variability survey (3 visits per night; $z_{AB} = 24$ , $y_{AB} = 22.6$ )					
Exposure time: $z$	15	48	30	10	216 ks
Exposure time: $y$	15	48	30	10	216 ks
Readout time	2	96	30	10	58 ks
Filter change	45	3	30	10	40.5 ks
Field totals: 1.67 Ms exposure, 0.172 Ms overhead					
Nightly average: 1.7 hr per night, 30 nights per year					

<sup>a</sup>Assuming one hour of DDF observations per night.

<sup>b</sup>Assuming an even split of 300 days among 10 DDF fields.

<sup>c</sup>The observations need not be spread over the specified number of years. We did the calculations assuming all 10 DDFs would be observed every single year. In fact, the photometric variability survey needs to be over 30 contiguous nights.

detections in the main LSST survey, the DDF observations need not go to this depth at multiple epochs but only for a single epoch. The proposed depth would allow LSST to detect L0 dwarfs to 3900 pc and T0 dwarfs to 450 pc in  $izy$ -filters (Figure 1), more than 3 and 1.5 times, respectively, as distant as the VIKING<sup>3</sup> J-band detection limits. These distance limits correspond to 15 (4.3) and 1.7 (0.50) times the thin (thick) disk scale height for L0 and T0 dwarfs (Bochanski et al. 2010), respectively, allowing an unambiguous detection of the density fall-off due to Galactic structure (even observing at a Galactic latitude of  $-30^\circ$ ).

As for the halo subdwarfs, we would need to go to  $g = 29$ – $30$ ,  $r = 27$ – $28$ , and  $i = 25$ – $26$  AB mags. Again, as these fields do not need to reimaged every year. While the expected observing time for a single field ( $\sim 270$  hrs per field) might seem prohibitive, the payoff for Galactic science would be immense. Moreover, the same science cannot be done with any other telescope.

The photometric variability part of our proposal requires  $\sim 70$ – $100$  observations over  $\sim 30$  days, equating to  $\sim 3$  visits per night over  $\sim 30$  days. As starspots evolve in similar timescales, the allotted nights need to be contiguous.

While we are not recommending further monitoring in the  $u$  band, we note that if other science goals need  $u$  band exposure, it will be very helpful for detecting flares ( $\Delta u \sim 4$  mag vs.  $\Delta g \sim 42$  mag for a typical M dwarf flare; Hilton et al. 2010) and constraining properties of white dwarfs.

## 2.4 Observation-Time Cost

We have summarized our accounting of the total LSST observation-time cost for our proposed fields in Tables 1, 2, and 3.

<sup>3</sup>VISTA Kilo-degree Infrared Galaxy survey; <http://www.eso.org/sci/observing/policies/PublicSurveys/sciencePublicSurveys.html#VISTA>

Table 2. Field 2 (Galactic Center)

	Time (s)	No. of exp. per night <sup>a</sup>	No. of nights per year <sup>b</sup>	No. of years per survey <sup>c</sup>	Total (ks)
Deep subdwarf survey (assuming $g_{AB} = 30$ , $r_{AB} = 28$ )					
Exposure time: $g$	120	25	30	10	900 ks
Exposure time: $r$	120	2	30	10	72 ks
Readout time	2	27	30	10	15 ks
Filter change	45	1	30	10	13.5 ks
Deep brown dwarf survey ( $i_{AB} = 28.9$ )					
Exposure time: $i$	120	25	30	3	270 ks
Readout time	2	25	30	3	4.5 ks
Field totals: 1.24 Ms exposure, 33 ks overhead					
Nightly average: 1.2 hr per night, 30 nights per year					

<sup>a</sup>Assuming one hour of DDF observations per night.

<sup>b</sup>Assuming an even split of 300 days among 10 DDF fields.

<sup>c</sup>The observations need not be spread over the specified number of years. We did the calculations assuming all 10 DDFs would be observed every single year. In fact, the photometric variability survey needs to be over 30 contiguous nights.

Table 3. Field 3 (Selected Open Cluster)

	Time (s)	No. of exp. per night <sup>a</sup>	No. of nights per year <sup>b</sup>	No. of years per survey <sup>c</sup>	Total (ks)
Deep brown dwarf survey ( $i_{AB} = 28.9$ )					
Exposure time: $i$ -band	120	25	30	3	270
Readout time	2	25	30	3	4.5
Photometric variability survey (3 visits per night; $z_{AB} = 24$ , $y_{AB} = 22.6$ )					
Exposure time: $z$	15	48	30	10	216
Exposure time: $y$	15	48	30	10	216
Readout time	2	96	30	10	58 ks
Filter change	45	3	30	10	40.5 ks
Field totals: 702 ks exposure, 103 ks overhead					
Nightly average: 45 min per night, 30 nights per year					

<sup>a</sup>Assuming one hour of DDF observations per night.

<sup>b</sup>Assuming an even split of 300 days among 10 DDF fields.

<sup>c</sup>The observations need not be spread over the specified number of years. We did the calculations assuming all 10 DDFs would be observed every single year. In fact, the photometric variability survey needs to be over 30 contiguous nights.

## 3 Other Required or Relevant Observations

### 3.1 Other Required Observations

Our science goals do not require further observations.

### 3.2 Other Relevant Observations

## 4 Specific Needs for LSST and for Deep Drilling

### 4.1 Need for LSST

Our Galactic targets include halo cool subdwarfs and substellar disk brown dwarfs, which are intrinsically the faintest isolated objects in the Galaxy. Although brown dwarfs have spectral energy distributions that peak in the near-infrared, the high backgrounds involved in ground-based NIR observations put upcoming surveys such as VIKING and UKIDSS LAS at a detection disadvantage to LSST. Additionally, L and T dwarfs are relatively blue in  $JHK$  colors due to molecular absorption features in the  $H$  and  $K$  bands, which makes them difficult to distinguish from the more numerous late-M dwarfs. The  $izy$  bands are ideal for L and T dwarf identification because their colors are simply redder with later spectral type (e.g., Schmidt et al. 2010). Detecting the fall-off of brown dwarfs with distance from the Galactic midplane is only possible with a large multi-band survey of exceptional depth due to their rarity—previous surveys using HST pencil-beams found fewer than one ultracool dwarf per pointing (Ryan et al. 2005). LSST will provide the large imaging area needed to find this sparse population at large distances, combined with the red-end sensitivity to detect and characterize them in multiple bands. The only possible competitors in this discovery space would be the expanded Pan-STARRS4 array (Kaiser et al. 2002) whose construction is somewhat in doubt; and even they would require a substantial time investment in order to replicate the DDF searches proposed here. The proper motions needed to separate halo and disk stars from each other and red extragalactic backgrounds will also be obtained by LSST over the course of the main survey, something very time-consuming to replicate with another instrument. The collecting area of LSST makes possible the extraordinarily deep imaging needed to search a new and exciting volume of the Galaxy in a reasonable period of time.

Between now and 2015, we expect the southern hemisphere to have been surveyed by the upcoming SkyMapper wide-area Southern Sky Survey to a depth comparable to SDSS (Keller et al. 2007), which will more than double the volume of the Solar Neighborhood searchable for brown dwarfs using 2MASS. In addition, we expect VIKING to have provided 1500 sq. deg. of  $J = 22.1$  (AB) survey imaging in the southern hemisphere, which will serve as a smaller, deeper complement to the UKIDSS  $J = 20.3$  (AB) Large Area Survey. However, neither survey will provide multi-band imaging to depths comparable to the main LSST survey or the DDF observations, which restricts the mapping of the lowest-mass members of the Milky Way.

For our open cluster targets, the advantages of LSST are clear: the large field of view samples the entire cluster at a single pass, while the large collecting area allows for rapid time-sampled measurements of rotation and weather variability on our brown dwarf targets, which would be impossible with a smaller telescope.

### 4.2 Need for Deep Drilling

For the subdwarf and brown dwarf targets, the essential advantage of the DDFs is depth. To identify our candidate objects, we need both astrometric information (which the LSST standard cadence survey will provide) and color information, which requires very deep observations in the bluer  $g$ ,

$r$ , and  $i$  filters. With DDF observations of the proposed fields, we can leverage the planned LSST survey imaging in  $z$  and  $y$  into more distant detections of rare disk and halo populations.

For the open clusters and for monitoring flares and clouds, the DDF has an equally critical advantage: frequent time-sampling. While some variable targets are assumed stable over long enough timescales that the standard cadence can be used to characterize them from sparse photometric series, the ultracool dwarfs in our open clusters have both predictable variability from rotation and gradual random changes from cloud changes and starspot activity. Observations separated by weeks or months, as may frequently be found in the LSST main survey, will be too poorly correlated to disentangle these multiple sources of variability. The rapid sampling of the DDF is the only way to extend the sensitivity of the main survey to shorter timescales and to lower-mass targets.

## 5 Feasibility

### 5.1 General Feasibility

The proposed DDF fields would result in a large database of the low-mass M, L, and T dwarfs that would extend to unprecedented Galactic heights and well into the Galactic halo. As these stars are the most abundant stellar constituents, we would be able to construct a comprehensive picture of the Milky Way's number density, velocity, and metallicity distributions. No current or proposed survey has a similar capability.

### 5.2 Bright Objects and Extinction

As two of our proposed fields are chosen to avoid the Galactic bulge and disk, there is no significant extinction/reddening along the lines-of-sight. Given the low stellar density, there should not be any issues with crowding and/or very bright objects, although there will be a handful of the latter. In a  $\sim 10$  sq. deg. field-of-view with thousands of stars, bleed trails from a few objects will not affect our science goals. The extinction/reddening along these lines-of-sight are very small.

While the proposed open cluster fields are closer to the Galactic disk, all three lines-of-sight are away from the Galactic Center. In addition the foreground reddening is small:  $\sim 0.1$  mag for IC 4651 and  $\sim 0.03$  mag for NGC 3532 and NGC 2527, according to the WEBDA database<sup>4</sup>.

### 5.3 Unresolved Feasibility Issues

There are no unresolved feasibility issues that we are aware of.

## 6 Other Issues

### 6.1 Relevance to LSST Commissioning

Our observations will develop the knowledge to identify MLT(Y) dwarfs at yet unexplored faintness and distances. Our observations would identify and characterize stellar sources and separate them from extragalactic sources when parallaxes and/or proper motions are not available. This would be of great value to the main LSST survey.

### 6.2 Other Relevant Information

## 7 References Cited

---

<sup>4</sup><http://www.univie.ac.at/webda/>

- Ackerman, A. S., & Marley, M. S. 2001, *ApJ*, 556, 872
- Allard, F., Hauschildt, P. H., Alexander, D. R., Tamanai, A., & Schweitzer, A. 2001, *ApJ*, 556, 357
- Bailer-Jones, C. A. L., & Mundt, R. 1999, *A&A*, 348, 800
- . 2001, *A&A*, 367, 218
- Barnes, S. A. 2003, *ApJ*, 586, 464
- . 2007, *ApJ*, 669, 1167
- . 2010, *ApJ*, 721
- Bochanski, J. J., Hawley, S. L., Covey, K. R., West, A. A., Reid, I. N., Golimowski, D. A., & Ivezić, Ž. 2010, *AJ*, 139, 2679
- Bond, N. A., et al. 2010, *ApJ*, 716, 1
- Browning, M. K. 2008, *ApJ*, 676, 1262
- Burrows, A., Hubbard, W. B., Lunine, J. I., & Liebert, J. 2001, *Reviews of Modern Physics*, 73, 719
- Burrows, A., Sudarsky, D., & Hubeny, I. 2006, *ApJ*, 640, 1063
- Chabrier, G., & Baraffe, I. 1997, *A&A*, 327, 1039
- Chiu, K., Fan, X., Leggett, S. K., Golimowski, D. A., Zheng, W., Geballe, T. R., Schneider, D. P., & Brinkmann, J. 2006, *AJ*, 131, 2722
- Cruz, K. L., et al. 2007, *AJ*, 133, 439
- Cruz, K. L., Reid, I. N., Liebert, J., Kirkpatrick, J. D., & Lowrance, P. J. 2003, *AJ*, 126, 2421
- Day-Jones, A. C., et al. 2011, *MNRAS*, 410, 705
- Deacon, N. R., Hambly, N. C., King, R. R., & McCaughrean, M. J. 2009, *MNRAS*, 394, 857
- Delfosse, X., Tinney, C. G., Forveille, T., Epchtein, N., Borsenberger, J., Fouqué, P., Kimeswenger, S., & Tiphène, D. 1999, *A&AS*, 135, 41
- Donati, J., et al. 2008, *MNRAS*, 390, 545
- Dupuy, T. J., Liu, M. C., & Bowler, B. P. 2009, *ApJ*, 706, 328
- Freytag, B., Allard, F., Ludwig, H., Homeier, D., & Steffen, M. 2010, *A&A*, 513, A19+
- Girardi, L., Bressan, A., Bertelli, G., & Chiosi, C. 2000, *A&AS*, 141, 371
- Gizis, J. E., Monet, D. G., Reid, I. N., Kirkpatrick, J. D., Liebert, J., & Williams, R. J. 2000, *AJ*, 120, 1085
- Goldman, B. 2005, *Astronomische Nachrichten*, 326, 1059
- Hawley, S. L., et al. 2002, *AJ*, 123, 3409
- Helling, C., Thi, W., Woitke, P., & Fridlund, M. 2006, *A&A*, 451, L9
- Helling, C., Woitke, P., & Thi, W. 2008, *A&A*, 485, 547
- Herbst, W., Bailer-Jones, C. A. L., & Mundt, R. 2001, *ApJ*, 554, L197
- Hilton, E. J., Hawley, S. L., Kowalski, A. F., & Holtzman, J. 2010, *ArXiv e-prints*
- Irwin, J., Berta, Z. K., Burke, C. J., Charbonneau, D., Nutzman, P., West, A. A., & Falco, E. E. 2011, *ApJ*, 727, 56
- Ivezić, Ž., et al. 2008, *ApJ*, 684, 287
- Kaiser, N., et al. 2002, in *Society of Photo-Optical Instrumentation Engineers (SPIE) Conference Series*, Vol. 4836, *Society of Photo-Optical Instrumentation Engineers (SPIE) Conference Series*, ed. J. A. Tyson & S. Wolff, 154–164
- Keller, S. C., et al. 2007, *PASA*, 24, 1
- Kirkpatrick, J. D., et al. 1999, *ApJ*, 519, 802
- . 2000, *AJ*, 120, 447
- Koen, C. 2003, *MNRAS*, 346, 473
- . 2005, *MNRAS*, 360, 1132
- Kowalski, A. F., Hawley, S. L., Hilton, E. J., Becker, A. C., West, A. A., Bochanski, J. J., & Sesar, B. 2009, *AJ*, 138, 633
- Lamm, M. H., Mundt, R., Bailer-Jones, C. A. L., & Herbst, W. 2005, *A&A*, 430, 1005
- Lépine, S., & Scholz, R.-D. 2008, *ApJ*, 681, L33
- Liebert, J., Kirkpatrick, J. D., Cruz, K. L., Reid, I. N., Burgasser, A., Tinney, C. G., & Gizis, J. E. 2003, *AJ*, 125, 343
- Liu, M. C., Dupuy, T. J., & Leggett, S. K. 2010, *ApJ*, 722, 311
- LSST Science Collaborations, et al. 2009, *ArXiv e-prints*
- Meibom, S., Mathieu, R. D., & Stassun, K. G. 2009, *ApJ*, 695, 679
- Mohanty, S., Basri, G., Shu, F., Allard, F., & Chabrier, G. 2002, *ApJ*, 571, 469
- Morin, J., et al. 2008, *MNRAS*, 390, 567
- Morin, J., Donati, J., Petit, P., Delfosse, X., Forveille, T., & Jardine, M. M. 2010, *MNRAS*, 407, 2269
- Oswalt, T. D., Smith, J. A., Wood, M. A., & Hintzen, P. 1996, *Nature*, 382, 692
- Pirzkal, N., et al. 2009, *ApJ*, 695, 1591
- . 2005, *ApJ*, 622, 319
- Prsa, A., Pepper, J., & Stassun, K. G. 2011, *AJ*, submitted
- Reid, I. N., et al. 2003, *AJ*, 126, 3007
- Reid, I. N., Cruz, K. L., Kirkpatrick, J. D., Allen, P. R., Mungall, F., Liebert, J., Lowrance, P., & Sweet, A. 2008, *AJ*, 136, 1290
- Reid, I. N., Kirkpatrick, J. D., Gizis, J. E., & Liebert, J. 1999, *ApJ*, 527, L105
- Reiners, A., & Basri, G. 2007, *ApJ*, 656, 1121
- . 2008, *ApJ*, 684, 1390
- Ryan, Jr., R. E., Hathi, N. P., Cohen, S. H., & Windhorst, R. A. 2005, *ApJ*, 631, L159
- Saumon, D., et al. 2007, *ApJ*, 656, 1136
- Schmidt, S. J., Cruz, K. L., Bongiorno, B. J., Liebert, J., & Reid, I. N. 2007, *AJ*, 133, 2258
- Schmidt, S. J., West, A. A., Hawley, S. L., & Pineda, J. S. 2010, *AJ*, 139, 1808
- Scholz, A., Eisloffel, J., & Mundt, R. 2009, *MNRAS*, 400, 1548
- Stassun, K. G., Mathieu, R. D., Mazeh, T., & Vrba, F. J. 1999, *AJ*, 117, 2941
- Stassun, K. G., Mathieu, R. D., & Valenti, J. A. 2006, *Nature*, 440, 311
- . 2007, *ApJ*, 664, 1154
- Thorén, P., Edvardsson, B., & Gustafsson, B. 2004, *A&A*, 425, 187
- Tinney, C. G., & Tolley, A. J. 1999, *MNRAS*, 304, 119
- West, A. A., Bochanski, J. J., Hawley, S. L., Cruz, K. L., Covey, K. R., Silvestri, N. M., Reid, I. N., & Liebert, J. 2006, *AJ*, 132, 2507
- West, A. A., Hawley, S. L., Bochanski, J. J., Covey, K. R., Reid, I. N., Dhital, S., Hilton, E. J., & Masuda, M. 2008, *AJ*, 135, 785
- West, A. A., et al. 2004, *AJ*, 128, 426
- . 2011, *AJ*, 141, 97
- Yi, S., Demarque, P., Kim, Y., Lee, Y., Ree, C. H., Lejeune, T., & Barnes, S. 2001, *ApJS*, 136, 417